N91-32644

Simulation and measurement of melting effects on metal sheets caused by direct lightning strikes

Alexander Kern
University of the Federal Armed Forces,
Munich Germany

Abstract

Direct lightning strikes melt metal parts of various systems, like fuel and propellant tanks of rockets and airplanes, at the point of strike. Responsible for this melting are the impulse current and, if occuring, the long duration current, both carrying a remarkable charge Q.

For studying these meltings the simulation in the laboratory has to be based on the parameters of natural lightnings. International standards exist defining certain threat levels of natural lightnings and giving possible generator circuits for the simulation.

The meltings caused by both types of lightning currents show different appearance. Their characteristics, their differences in melting and heating of metal sheets are investigated.

Nevertheless the simulation of lightning in the laboratory is imperfect. While natural lightning is a discharge without a counter electrode, the simulation always demands a close counter electrode. The influence of this counter electrode is studied.

1. Introduction

Metal sheets as parts of various systems can be exposed to direct lightning strikes, e.g. fuel and propellant tanks of rockets and airplanes.

Direct lightning strikes may cause melting effects on metal sheets up to burn throughs. But even if the metal is thick enough to withstand puncturing, the temperature rise at the opposite side of the metal sheet, i.e. the inner side of a tank, may be high enough to ignite explosive mixtures.

Responsible for this heating resp. melting effect is mostly the charge Q. From Q, multiplied by the nearly constant anode or cathode voltage drop, results the energy converted at the point of strike.

The two components of a natural lightning strike carrying a significant charge Q are the impulse current and, if it occurs, the long duration current. If one wants to simulate those heating or melting effects, the simulation has to be very close to natural lightning, i.e. the simulated impulse and long duration currents have to correspond to the components of natural lightnings as far as possible.

In the past years a lot of efforts were done from the International Electrotechnical Commission (IEC), to work out definitions for the threat of natural lightnings. At the October 1990 - meeting of the Technical Committee 81 (TC 81) of IEC the parameters have been finally concluded /1/. Now these definitions are accepted internationally, and they will be obligatory for standards for lightning protection.

In this paper generators are presented, which are able to fulfil the definitions given by IEC TC 81: an impulse current generator with a double-crowbar sparkgap and a long duration current generator. Both generators are realized at the High Voltage Laboratory of the University of the Federal Armed Forces in Munich, Germany.

With these generators experiments have been performed at different metal sheets made of copper, aluminium, brass and two kinds of steels. The differences in the meltings on these metal sheets caused by impulse currents and long duration currents are presented. The melting effects are discussed as a function of the kind of metal, the thickness of the sheets and the parameters Q (charge) and W/R (specific energy) of the lightning current.

Natural lightning is a discharge without a nearby counter electrode, while in the laboratory simulation there always has to be a rather close counter electrode. Therefore the influence of the distance between the test sample and the counter electrode and the geometrical form of the counter electrode are especially investigated.

If the metal sheet is thick enough to withstand puncturing by the lightning current, measurements of the heating at the opposite side of the sheet are conducted with infrared thermosensors. These measurements conclude the time slope and the maximum value of the temperature at the hottest point of the sheet's opposite side, i.e. directly behind the point of strike of the electric arc.

2. Natural lightnings

For analysis and for classification of lightning currents four threat parameters are defined characterizing specific effects of lightning:

- Peak current i_{max}, responsible for the ohmic voltage drops of stroken objects.
- Charge $Q = \int i\,dt$, leading to melting, vaporizing and welding by the electric arc at the point of strike. Because of the different effects the total charge Q_t has to be divided into the charge of the impulse current Q_i and the charge of the long duration current Q_l.
- Specific energy $W/R = \int i^2 dt$, also called the action integral, responsible for the heating and the electrodynamic forces of metal wires carrying the lightning current.
- Current rate-of-rise $\Delta i/\Delta t$ in the front of a lightning current, leading to electromagnetically induced voltages in installation circuits.

About ten years ago the measurements of natural lightning currents, which were available worldwide, were taken together. Then the data were statistically prepared, related to the four defined threat parameters. This work was conducted by the Working Group 33 of the International Conference On Large High Voltage Electric Systems (CIGRE WG 33) /2, 3/.

The basic results of that work are shown in fig. 1 to 4, seperated for negative first strokes, negative following strokes and positive flashes. The figures give the frequency distribution of the peak current i_{max}, the total charge Q_t, the impulse charge Q_i and the specific energy W/R, those threat parameters, which are necessary to define impulse and long duration currents for the laboratory simulation. The distribution of the current rate-of-rise $\Delta i/\Delta t$ is not shown in this paper, because this parameter does not have a remarkable influence on melting or heating effects.

3. Standards for the laboratory simulation

Standards for the simulation of lightning currents in the laboratory have to be based on the parameters of natural lightnings given in chapter 2. At first one has to define a certain protection level for the device under test. IEC TC 81 fixes four protection levels, which can be chosen /1/. The highest level, protection level "I", includes about 99% of all natural lightnings, i.e. only 1% of natural lightnings exceeds the defined current parameters.

The german military standard VG 96 901 Teil 4 /4/, valid for planning and construction of systems and equipment for the Bundeswehr, corresponds to the definitions of IEC. Two threat levels are determined here: threat level "high" also includes about 99% of natural lightnings, threat level "normal" about 95%.

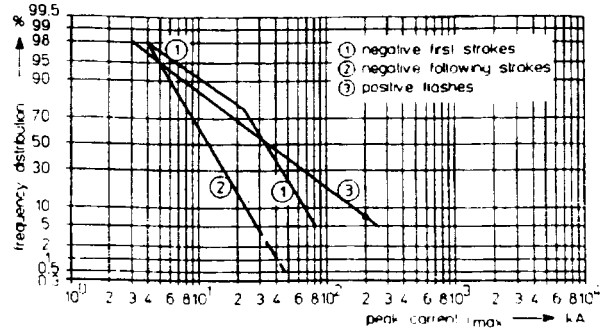

Fig. 1 Frequency distribution of the peak current i_{max}

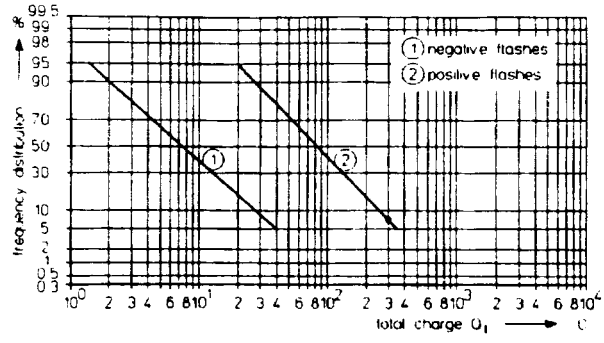

Fig. 2 Frequency distribution of the lightning total charge Q_t

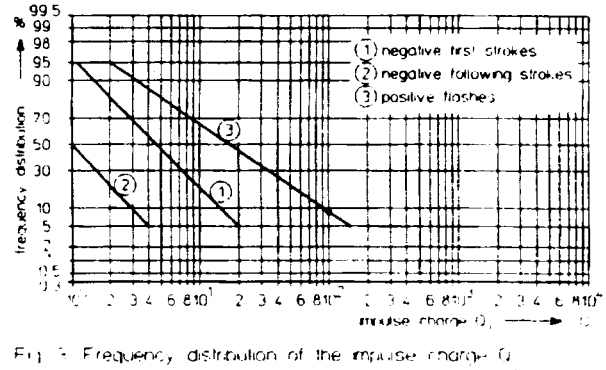

Fig. 3 Frequency distribution of the impulse charge Q_i

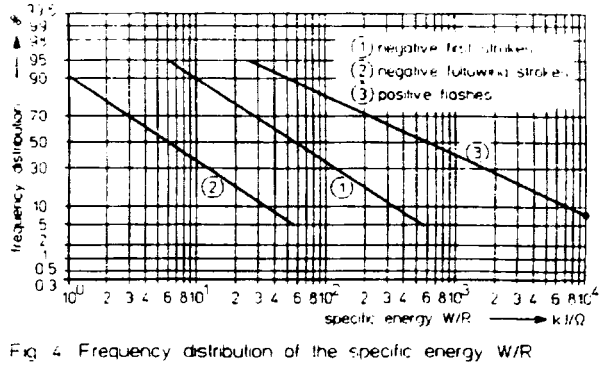

Fig. 4 Frequency distribution of the specific energy W/R

If the protection resp. threat level is fixed, one can go into the statistical data. There one gets the current parameters for the chosen level. It is important, that all parameters for a simulated lightning current are based on the same protection level. For example, if a impulse current for protection level "I" shall be simulated, all current parameters, in this case the peak current i_{max}, the impulse charge Q_i and the specific energy W/R, have to fulfil the 99%-value.

Furthermore for accurate reading of the current parameters in the statistical data it has to be taken into account, that about 10% of natural lightnings are positive flashes. So for the fixing of the current parameters the influence of these positive flashes must be included with appropriate importance.

Responsible for the heating resp. melting effects on metal sheets are two components of a natural lightning current, the impulse and the long duration current. Based on the above considerations the following parameters are fixed for protection level "I" of IEC /1/ resp. threat level "high" of VG 96 901 Teil 4 /4/:

- impulse current
  peak current i_{max} = 200 kA ± 10%
  charge Q_i = 100 C ± 20%
  specific energy W/R = $\int i^2 dt$ = 10 MJ/Ω ± 35%

- long duration current
  charge Q_l = 200 C ± 20%
  time T_l = 0,5 s ± 10%

The experimental investigations published in this paper are conducted with currents fulfilling these parameters, which, as mentioned before, include about 99% of natural lightnings.

The aviation industry normally uses another standard for the simulation of lightning currents, the SAE AE4L /5/ resp. the MIL-STD 1757A /6/. These standards define a long duration current, which corresponds to the definitions of IEC, but the impulse current shows remarkable differences.

This impulse current has a peak current i_{max} of 200 kA, an impulse charge Q_i of 20 C, which is increased by an intermediate current up to 30 C, and a specific energy W/R of 2 MJ/Ω. Using the statistical data of chapter 2, the current parameters can be analyzed:

- The peak current i_{max} includes about 99% of natural lightnings, like required by IEC for protection level "I".

- The impulse charge Q_i corresponds only to the 90%-value of natural lightnings (95% of first negative strokes, 50% of positive flashes). If the charge of the intermediate current is added, it corresponds to the 94%-value.

- The specific energy W/R includes about 96% of natural lightnings. In fact the defined value of 2 MJ/Ω considers about 99% of the first negative strokes /7/, but only about 70% of the positive flashes, which absolutely may not be forgotten.

The impulse current fixed in SAE AE4L resp. MIL-STD 1757A shows parameters, which are not correlated in relation to the probability of appearance in the reality. It simulates natural lightnings only incompletely.

So if one wants to simulate the real threat of natural lightnings, the parameters given by IEC have to be taken. In the future it can be expected, that more and more national and international standards will be based on the definitions of IEC.

4. Laboratory equipment

4.1 Impulse current generator

For the simulation of impulse currents with peak currents in the range of some 100 kA mostly capacitive surge current generators are used. Especially for the simulation of extreme values of charge and specific energy, as demanded in /1, 4/, a capacitive surge current generator with a crowbar sparkgap is of great advantage. As shown in /8/, with the crowbar technique it is possible to achieve a charge transfer through the device under test, which is up to a factor of 40 greater than the stored charge in the capacitor bank. Thus the capacitor bank can be kept relatively small.

The costs of a surge current generator are dominated by the prize of the capacitor bank. Therefore the equipment should be used as efficient as possible. A further improvement of the efficient use of a given capacitor bank can be realized by seperating the whole test equipment into two identical parts, each with its own crowbar sparkgap. The two parts of the generator are only connected by the device under test, where their currents are summarized.

Compared with a single surge current generator of the same total surge capacitance and the same charging voltage the peak current i_{max} as well as the impulse charge Q_i achieved in such a twin arrangement are greater according to a factor $\sqrt{2}$, the specific energy W/R according to a factor 2 /9/.

The equivalent circuit of a twin arranged surge current generator is shown in fig. 5.

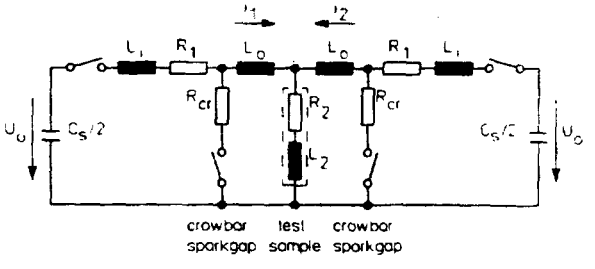

U_0 charging voltage
C_s capacitor bank
L_1 internal inductance (of the capacitor bank)
R_1 damping resistance
L_2 inductance of the test sample
R_2 resistance of the test sample
L_0 magnetic storage element
R_{cr} non linear resistance of the crowbar sparkgap

Fig 5 Twin arrangement of a surge current generator

The decay time constant τ_1 of the exponential decay of the current is given by

$$\tau_1 = (L_0 + 2 \cdot L_2)/(R_{cr} + 2 \cdot R_2).$$

The parameters of the current can be calculated according to the following equations:

$$Q_i \approx i_{max} \cdot \tau_1; \; W/R \approx i_{max}^2 \cdot \tau_1/2$$

$$i_{max} = U_0 \cdot \sqrt{\frac{C_s}{L}} \cdot \eta; \; \eta = \exp\left(-\frac{\mathrm{Atn}(\omega \cdot \tau)}{\omega \cdot \tau}\right)$$

$$L = \frac{L_o + L_i}{2} + L_2;\ R = \frac{R_1}{2} + R_2$$

$$\tau = \frac{2L}{R};\quad \omega = \sqrt{\frac{1}{L \cdot C_s} - \frac{1}{\tau^2}}$$

The realization of a twin arranged surge current generator for the simulation of the impulse current according to /1, 4/ is shown in fig. 6. A typical current obtained with this equipment and a sparkgap with a spacing of 20 mm as test sample is given by fig. 7.

The use of a surge current generator in a twin arrangement has a further significant advantage, if melting or heating effects are to be studied. Because of the geometric symmetry the magnetic fields and the resulting magnetic forces of both generator parts are neutralized at the position of the test sample. Thus the arc in the test sample burns uninfluenzed by the external magnetic fields caused by the leads to the test generator. This situation corresponds to the impact mechanism of a natural lightning strike to a metal sheet.

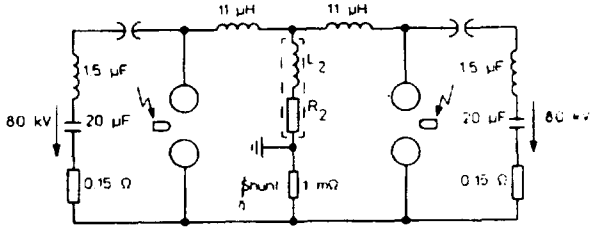

Fig. 6 Twin arranged surge current generator with two crowbar sparkgaps

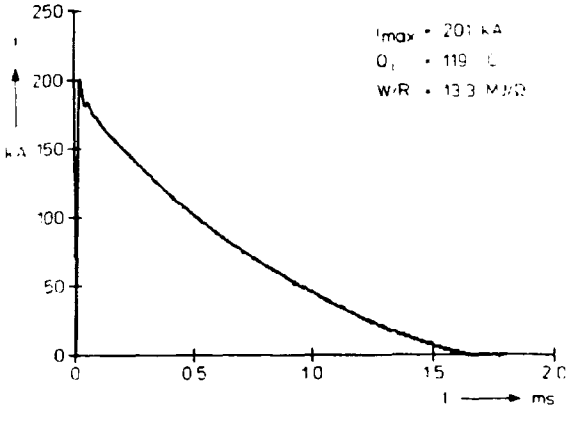

Fig. 7 Typical impulse current

4.2 Long duration current generator

For the simulation of the long duration current another capacitor bank is used. The circuit is shown in fig. 8.

The control unit creates the triggering impulses for both thyristors V regulating the primary transformer current. On the secondary side of the transformer the voltage is demodulated by the d.c.-converter. The capacitor bank C is charged on this direct voltage.

After the long duration current has been triggered, the capacitor bank feeds in the test sample over an electric arc. While the current flows, the capacitor bank is permanently recharged by the transformer via the d.c.-converter. With this arrangement the long duration current of fig. 9 with nearly rectangular wave shape is generated.

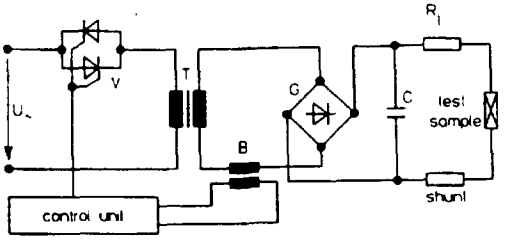

$U_\sim$ alternating voltage 220 V
V thyristors
T transformer 220/400 V
B current transformer
G d.c.-converter
C capacitor bank 41.3 mF
R_1 loading resistor

Fig. 8 Long duration current generator

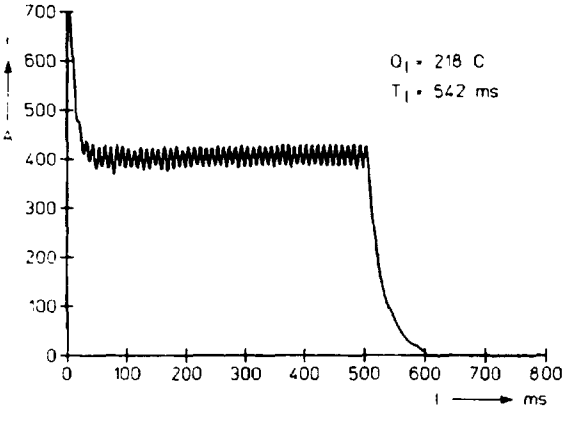

Fig. 9 Typical long duration current

The current amplitude is fixed by the output voltage of the capacitance and the resistance in the circuit. The total resistance consists of the resistances of the test sample, the electric arc, the shunt and the loading resistor R_1. With this adjustable loading resistor different current amplitudes can be created at constant transformer resp. capacitance voltage.

The secondary 50 Hz-half waves behind the transformer are counted with the current transformer B. After a certain time duration, which has to be fixed at the control unit previously, no more triggering impulses for the thyristors are created. The primary and therefore also the secondary transformer current are blocked, and the capacitor bank is discharged exponentially via the test sample.

5. Melting effects

For the tests on metal sheets the following typical materials were selected:

- aluminium
- copper
- brass
- soft steel (St37)
- stainless steel (V2A)

5.1 Impulse currents

The melting effects on metal sheets caused by impulse currents have a typical appearance. The melted material is spread over a large area with diameters of several cm up to 10 cm. Some examples of melting caused by impulse currents are shown in fig. 18 and 19. The melted areas are surrounded by a zone of splashed material.

The radius of the melted area depends on the kind of material. Sheets of soft and stainless steel show the largest melted areas (typ. 8 cm), followed by aluminium sheets (typ. 6 cm), brass and copper (typ. 4 to 5 cm). The depth of those melted areas is very small. It ranges from 0.1 to 0.2 mm, for aluminium up to 0.4 mm.

The comparatively large melted areas result from the high specific energy (which is equal to $\int i^2 dt$) of the impulse current. This specific energy is responsible for the electrodynamic forces. The melted areas found at the tests with long duration currents, which have a considerably lower specific energy, are remarkably smaller (typ. 1..2 cm).

The spacing and the geometrical construction of the counter electrode does not affect the diameter of the melted area.

5.1.1 Test performance

The decay time constant τ_1 of the current and as a consequence the impulse charge Q_i are a function of the resistance in the circuit. If the distance between the counter electrode and the test sample increases, the resistance of the electric arc and therefore the total resistance in the circuit rises. The attitudes of the decay time constant τ_1 and the charge Q_i as a function of the spacing of the counter electrode are shown in Fig. 10 and 11. The charging voltage here was fixed at 80 kV.

The results allow a rough calculation of the arc's resistance. Comparing the different decay time constants τ_1 or the charges Q_i according to the equations of 4.1, the resistance of the electric arc related to it's length is approximately

$R' = 0{,}75\ m\Omega/cm$.

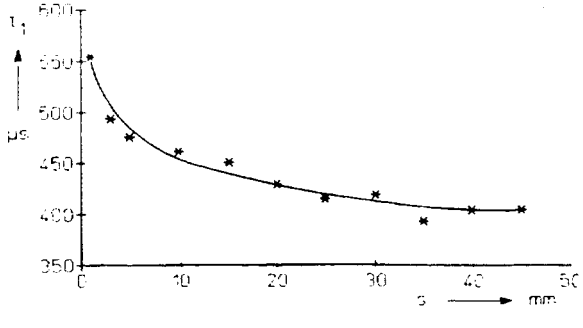

Fig. 10 Decay time constant τ_1 as a function of the spacing s of the counter electrode

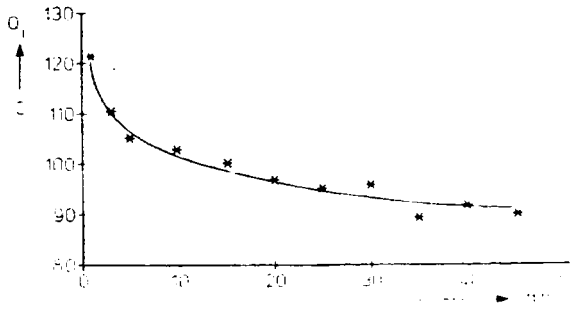

Fig. 11 Impulse charge Q_i as a function of the spacing s of the counter electrode

This relation is only valid for arcs of currents in the range of 200 kA. Furthermore the anode and cathode voltage drop is not considered in this relation. In the investigated case the value of this voltage can be estimated to $U_{A,K} \approx 30$ V.

To make comparable measurements the charging voltage was accommodated to the spacing of the counter electrode. The resulting charge Q_i could be kept constant within 5% (Q_i = 100 ± 5 C).

To eliminate the remaining differences, the values were corrected linearly to Q_i = 100 C.

5.1.2 Test results

The spacing between the counter electrode and the test sample affects the melting loss in material. An increasing distance drags a decreasing value for the loss in volume.

Melted and splashed material is a result of the formation of plasma rays between the sheets and the counter electrode. The larger their spacing, the weaker the influence of the plasma rays at the surface of the sheets and the fewer their power to melt and to splash the material.

A simple way to eliminiate the power of those plasma rays as far as possible is the use of a so called insulating electrode (electrode II), like shown in fig. 12.

In contrast to the standard electrode (electrode I) this insulating electrode has a teflon cap at its top. With this the electric arc is forced to leave the electrode radially and to "curve" to the test device. The plasma rays also leave the electrode radially, and therefore they do not strike the test device with the same power as known from electrode I.

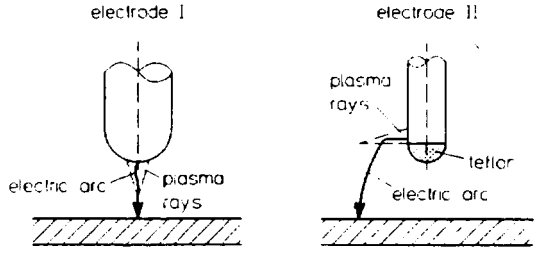

Fig. 12 Construction of two counter electrodes

The tests were conducted with the five chosen metals and for both electrodes. The losses in volume ΔV as a function of the spacing s of the electrode are shown in fig. 13 to 17.

Different materials show different values of the loss in volume. The specified losses of the different materials are a function of the melting and boiling temperatures and of the thermal capacities and conductivities. The higher the temperatures, the capacities and conductivities, the smaller the loss in volume.

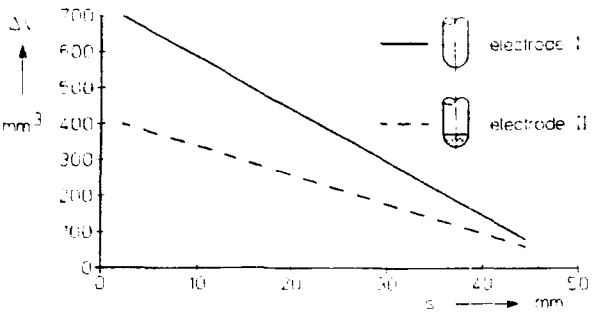

Fig. 13 Loss in volume ΔV of aluminium

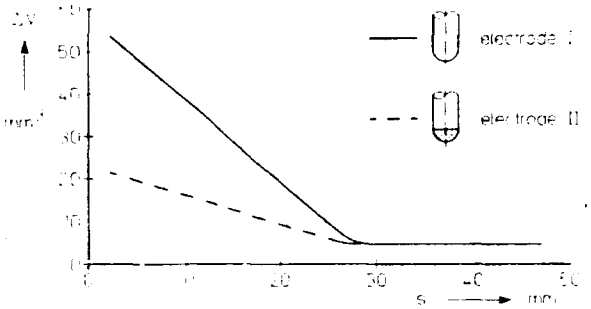

Fig. 14 Loss in volume ΔV of copper

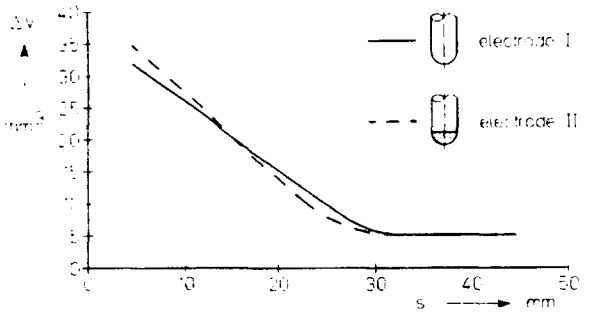

Fig. 15 Loss in volume ΔV of brass

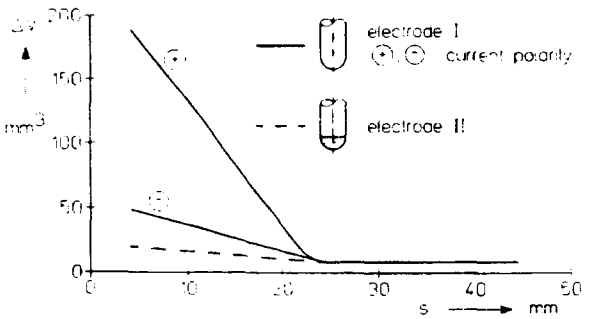

Fig. 16 Loss in volume ΔV of soft steel

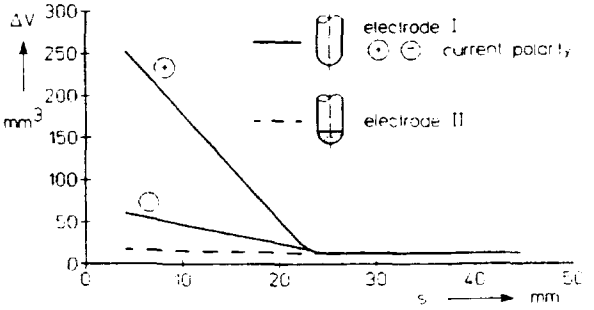

Fig. 17 Loss in volume ΔV of stainless steel

The loss in volume is independent of the impulse current's polarity, excepted steel sheets. For both steels the values for positive polarity are four times greater than for negative, if the standard electrode I is used. The loss in volume is dominant at the cathode. It can be assumed, that the plasma rays starting from the anode are "stronger" than those starting from the cathode. The same phenomenon occured at tests with safety gaps for overvoltage protection made of stainless steel /8/. Here meltings at the cathode were dominant, too. For electrode II there is no remarkable difference between anodic or cathodic meltings.

The losses in volume depend on the spacing of the counter electrode. The larger the spacing, the smaller the loss. This is valid up to a spacing of about 25 mm. Then a minimum value for the loss in volume of 5 to 10 mm^3 is reached, remaining constant for larger spacings. However, for aluminium this minimum value can only be seen for spacings of more than 45 mm. Reason for this is probably the softness of aluminium, which allows an easier splashing of melted material. The common minimum value for all investigated metals of not more than 10 mm^3 should be that part of the material vaporizing at the point of strike.

The comparison of the losses in volume for both electrodes leads to different results. For brass there is no significant influence; copper and aluminium show values for electrode II, which are only 40% to 60% of the values measured for electrode I. However, for the steels the reducing effect of electrode II is very high. The loss in volume is minimized to not more than 20 mm^3.

As mentioned before, the reason for this results is, that the influence of the plasma rays on the metal sheet is remarkably smaller for electrode II. The remaining differences between the investigated metals, especially for aluminium, are caused by their different softness.

The thickness d of the sheets affects their resistance. However, though the resistance of the circuit increases with thinner sheets, the influence on the decay time constant τ_1 and the impulse charge Q_i is unimportant. Also the loss in volume is not influenced by the thickness of the test samples.

5.1.3 Theoretical analysis

A theoretical description of the loss in volume as a function of charge and specific energy is given in /8/:

$$\Delta V = C_1 \cdot Q_i^{C_2} \cdot (W/R)^{C_3},$$

with C_1, C_2 and C_3 as parameters typical for the material, the impulse charge in C, the specific energy in J/Ω and the volume ΔV in mm^3. This equation was developed for safety gaps for overvoltage protection /8/, but the experimental results with metal sheets show a comparable relation.

The experimental results allow also an extension of this equation. The loss in volume decreases with increasing spacing of the counter electrode:

$$\Delta V \sim (1 - C_4 \cdot s).$$

This relation is verified for a spacing of 1 mm up to 25 mm (resp. 1 mm and 45 mm for aluminium). The complete equation for the description of the loss in volume can be written as

$$\Delta V = C_1 \cdot Q_i^{C_2} \cdot (W/R)^{C_3} \cdot (1 - C_4 \cdot s),$$

with the spacing s in mm. The parameters C_1 and C_4 depend on the different materials and the used electrode (table 1 and 2), whereas C_2 and C_3 are valid for all investigated materials:

$C_2 = 1,4$
$C_3 = 0,45.$

5.2 Long duration currents

The meltings caused by long duration currents show a typical appearance, too. The diameter of the melted area is smaller, the melting itself deeper than in the case of impulse currents. Examples of these meltings are shown in fig. 20 and 21.

Using the long duration currents carrying a charge Q_l = 200 C according to /1, 4/, the diameter of the melted area is larger for the steels and aluminium (typ. 2 cm) than for brass and copper (typ. 1 cm).

These relatively small melted areas result from the smaller specific energy (action integral $\int i^2 dt$) of the long duration current. This is also the reason, that a measurement of the loss in volume, comparable to the tests with impulse currents, is impossible. The material is melted at the base of the electric arc, but not splashed significantly. Therefore the melted material hardens again, if the current flow is over. The loss in volume is nearly equal to 0.

So the measurements concentrate on the investigation, which thickness of a metal sheet can withstand the long duration current without being punctured. International and national standards define minimum thicknesses of different materials, if direct lightning strikes are assumed. The CO paper of IEC TC 81 /10/ for instance fixes:

- aluminium: 7 mm
- copper: 5 mm
- steel: 4 mm.

C_1	$* 10^{-6}\ mm^3/A^{2,3} * s^{1,85}$	
	electrode I	electrode II
aluminium	800	450
copper	70	30
brass	40	45
soft steel ⊕	250	25
soft steel ⊖	60	25
stainless steel ⊕	350	25
stainless steel ⊖	90	25

Table 1 Parameter C_1 for different metals

C_4	mm^{-1}	
	electrode I	electrode II
aluminium	0.020	0.020
copper	0.033	0.030
brass	0.030	0.033
soft steel	0.035	0.020
stainless steel	0.037	0

Table 2 Parameter C_4 for different metals, valid up to a spacing of 25 mm (aluminium 45 mm)

The experimental results show, that aluminium sheets can be punctured up to a thickness of 3 mm, the steels, brass and copper up to 2,5 mm, but for these thicknesses the occurence of puncturing is not sure. For example the 3 mm aluminium sheet is punctured only with a probability of 25%. The thicknesses of sheets, which are surely punctured, are given in table 3, together with the diameter of the occuring hole /11/. Sheets being 1 mm thicker than the values of table 3 are surely not punctured.

metal	d (mm)	h (mm)
aluminium	2.5	5 - 13
copper	2.0	4 - 10
brass	2.0	4 - 10
soft steel	2.0	6 - 12
stainless steel	2.0	6 - 12

Table 3 Thicknesses d and hole diameters h of metal sheets being surely punctured by a long duration current with Q_l = 200 C

Both electrodes are used for these tests, and their spacing is varied. Nevertheless the appearence of the melted areas, the possibility of puncturing the metal sheets and the current parameters are not affected by the different spacing and the kind of electrode.

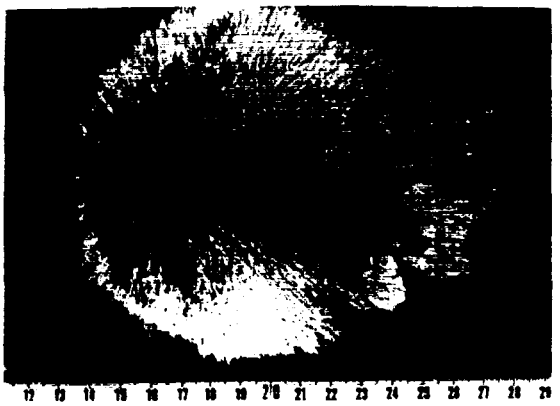

Fig. 18 Typical melting of aluminium sheet caused by impulse current (thickness d = 1.5 mm)

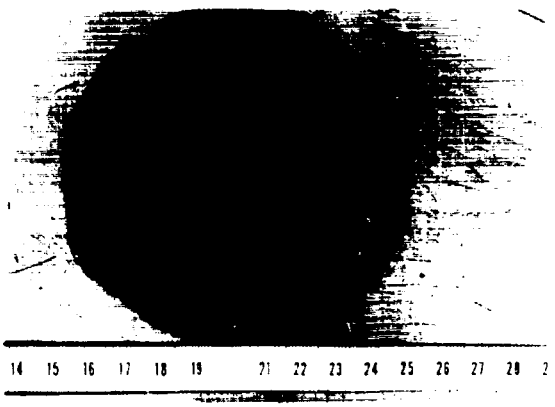

Fig. 19 Typical melting of stainless steel sheet caused by impulse current (d = 1.5 mm)

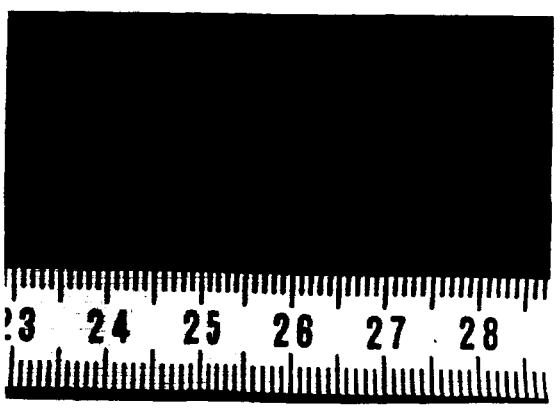

Fig. 20 Typical melting of aluminium sheet caused by long duration current (d = 2.0 mm)

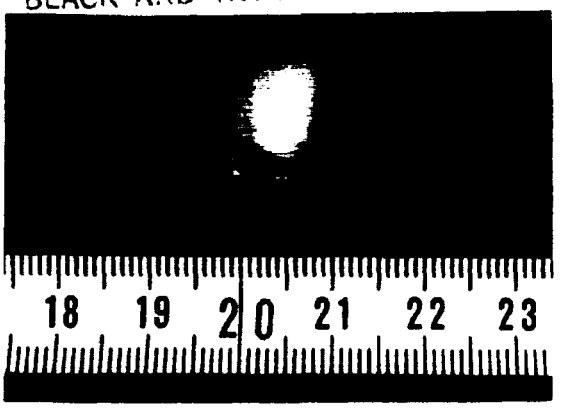

Fig. 21 Typical melting of stainless steel sheet caused by long duration current (d = 1.5 mm)

6. Temperature distributions

For metal sheets, which are thick enough that they can't be punctured, another thermal effect has to be investigated: the temperature rise at the interior surface. The temperatures occuring at the sheet opposite to the point of strike are high enough to decolorate the metal. These high temperatures can lead to an ignition of an explosive mixture inside a metal tank struck by lightning.

The time dependent temperatures at the interior surface of metal sheets are measured by two infrared thermosensors for different temperatur ranges with rise times of 250 ms resp. 550 ms. Therefore only relatively slow temperature rises can be measured exactly.

The test assembly is shown principly in fig. 22. The infrared thermosensor is adjusted to that point of the sheet opposite to the point of strike, i.e. in the axis of the counter electrode. At this point the highest temperatures occur.

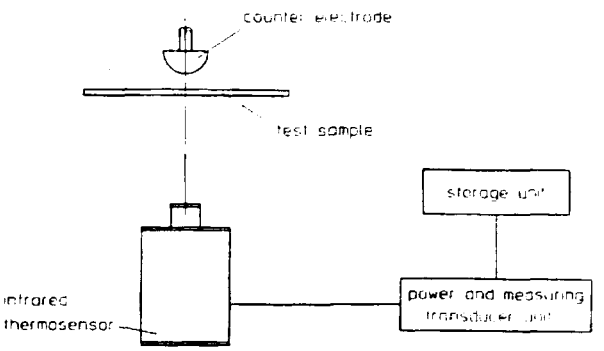

Fig. 22 Temperature measurement assembly

The radius of the detected area is proportional to the distance between thermosensor and the sheet. For thermosensor I the used distance of 30 cm corresponds to an area's radius of 10 mm; thermosensor II detects an area with the radius 3 mm. With this arrangement the integrated temperatures of two detected areas with the same center but different radius are recorded.

It has to be considered, that the temperatures in the middle of the detected area are normally still higher than the integrated temperatures. Based on the measurement results, however, a numerical model allows the calculation of the temperatures at each point of the metal sheet /11/.

The emission coefficient ϵ of the investigated metals is smaller than 1. Therefore the measured temperatures T_m in K have to be translated in the real temperatures T_r according to the equation

$$T_r^4 = \frac{T_m^4 - (1 - \epsilon) \cdot T_o^4}{\epsilon}$$

with T_o being the ambient temperature, usually 293 K.

The temperature rise of metal sheets caused by impulse currents is relatively fast, but after reaching the maximum temperature the tail of the curve is very even. Though the thermosensor isn't able to follow the front steepness exactly, the maximum temperature and the tail can be measured sufficiently. The maximum temperatures for sheets with a thickness of 2 mm are given in table 4.

metal	ϑ_{max} (°C)
aluminium	103
copper	68
brass	62
soft steel	94
stainless steel	105

Table 4 Maximum temperatures ϑ_{max} for 2 mm metal sheets caused by impulse currents

These temperatures were measured only with the thermosensor detecting an area with a radius of 10 mm, because the minimum temperature for the second thermosensor is 400°C. So the use of the second thermosensor was not possible, because of the relatively low temperatures of not more than about 100°C. The reason for those low temperatures are the large melted areas with only a small depth caused by the impulse currents.

The temperatures for sheets struck by long duration currents show a different time slope. The crest values are many times higher, and the tail is much shorter. So the thermosensors aren't able to follow the time dependent temperatures for all metals exactly. Only the steel sheets show temperature distributions, which are slow enough, to fulfil the measurement requirements, and so the investigations have to be limited to them.

The recorded temperatures with time constants for steel sheets with different thicknesses are shown in table 5. Both thermosensors were used and therefore the radius of the detected area is different. These relatively high temperatures are caused by the deep melted areas at the point of strike of long duration currents.

metal	z (mm)	r (mm)	ϑ_{max} (°C)	T_{cr} (s)	T_2 (s)
soft steel	3	3	1 120	0.7	2.7
		10	740	1.1	6.0
	4	3	950	1.0	--
		10	540	1.4	6.2
	5	3	750	1.4	--
		10	430	1.7	6.4
stainless steel	3	3	1 150	0.8	3.5
		10	550	1.0	10.5
	4	3	940	1.3	--
		10	400	1.8	10.0
	5	3	570	1.7	--
		10	270	2.7	13.4

z thickness of sheet

r radius of detected area

ϑ_{max} maximum temperature

T_{cr} time to crest

T_2 decay time to half value

Table 5 Temperature distributions for metal sheets caused by long duration currents

7. Conclusions

The simulation of lightning currents in the laboratory has to be based on the parameters of natural lightnings. The investigations of this paper are carried out with simulated lightning currents including about 99% of natural lightnings, as required by IEC /1/.

Meltings of metal sheets caused by impulse currents show a large melted area. The depth of the melting is small. The reason for this kind of melting is the high specific energy of the impulse current.

The loss in volume decreases with increasing spacing of the counter electrode due to the weaker influence of plasma rays on the metal sheet. If a so called insulating electrode is used, the influence of plasma rays and therefore also the loss in volume is reduced remarkably.

Meltings of metal sheets caused by long duration currents show a small, but deep melted area. Aluminium sheets can be punctured up to a thickness of 3 mm, stainless and soft steel, brass and copper up to 2,5 mm.

Metal sheets, which can't be punctured, can show high temperatures at their interior surface, i.e. opposite to the point of strike. Responsible for this are mainly long duration currents. They lead to maximum temperatures of more than 1.000°C, whereas the temperatures for impulse currents usually are below 100°C. Reason for these different temperatures are also the different melting processes of impulse and long duration currents.

Steel sheets show the most "dangerous" temperature distributions, because high temperatures occur at the interior surface of the sheets for a long time. The temperature decrease of sheets made of aluminium, copper and brass is faster.

In general it is a fact, that the thermal threat for metal sheets caused by long duration currents is dominant. They lead to deeper meltings and higher temperatures at the interior surface of the sheets than impulse currents.

References:

/1/ CEI/IEC 1024-1(1990-03): Lightning protection of structures. Part I: General principles.

/2/ Berger, K.; Anderson R.B.; Kröninger H.: Parameters of lightning flashes. Electra 41(1975), p. 23-37.

/3/ Anderson R.B.; Eriksson A.J.: Lightning parameters for engineering application. Electra 69(1980), p. 65-102.

/4/ VG 96 901 Teil 4/10.85: Schutz gegen Nuklear-Elektromagnetischen Impuls (NEMP) und Blitzschlag; Allgemeine Grundlagen, Bedrohungsdaten. Beuth Verlag, Köln.

/5/ SAE AE4L: Protection of aircraft electrical/electronic systems against the indirect effects of lightning. Committee report, 4. Feb. 1987.

/6/ MIL-STD 1757A: Lightning qualification test techniques for aerospace vehicles and hardware.

/7/ Melander B.G.: Atmospheric electricity threat definition for aircraft lightning protection. 8th. Int. Conf. on Lightning and Static Electricity, Fort Worth, Texas, 1983, Paper 36.

/8/ Zischank W.: Schutzfunkenstrecken zur Überspannungsbegrenzung bei direkten Blitzeinschlägen. Diss. Hochschule der Bundeswehr München, 1983.

/9/ Zischank W.: A surge current generator with a double-crowbar sparkgap for the simulation of direct lightning stroke effects. ISH Braunschweig, 1987, Paper No. 61.07.

/10/ IEC TC 81; CO paper 4/87: Standards for lightning protection of structures. Part I: General principles.

/11/ Kern A.: Theoretische und experimentelle Untersuchung der Erwärmung von Metallblechen bei Blitzeinschlag. Diss. Universität der Bundeswehr München, 1990.

Adress of author:

Dr.-Ing. A. Kern
Universität der Bundeswehr München
ET / 7
Werner-Heisenberg-Weg 39
D-8014 N e u b i b e r g